Developmental Cell
Article

Planar Cell Polarity Protein Celsr1 Regulates Endothelial Adherens Junctions and Directed Cell Rearrangements during Valve Morphogenesis

Florence Tatin,[1] Andrea Taddei,[1] Anne Weston,[2] Elaine Fuchs,[3] Danelle Devenport,[4] Fadel Tissir,[5] and Taija Makinen[1,*]
[1]Lymphatic Development Laboratory
[2]Electron Microscopy Unit
Cancer Research UK London Research Institute, 44 Lincoln's Inn Fields, London WC2A 3LY, UK
[3]Laboratory of Mammalian Cell Biology and Development, Howard Hughes Medical Institute, The Rockefeller University, 1230 York Avenue, Box 300, New York, NY 10065, USA
[4]Department of Molecular Biology, Princeton University, 119 Lewis Thomas Labs, Washington Road, Princeton, NJ 08544, USA
[5]Institute of Neuroscience, Developmental Neurobiology, Université Catholique de Louvain, B1200 Brussels, Belgium
*Correspondence: taija.makinen@cancer.org.uk
http://dx.doi.org/10.1016/j.devcel.2013.05.015

SUMMARY

Planar cell polarity (PCP) signaling controls tissue morphogenesis by coordinating collective cell behaviors. We show a critical role for the core PCP proteins Celsr1 and Vangl2 in the complex morphogenetic process of intraluminal valve formation in lymphatic vessels. We found that valve-forming endothelial cells undergo elongation, reorientation, and collective migration into the vessel lumen as they initiate valve leaflet formation. During this process, Celsr1 and Vangl2 are recruited from endothelial filopodia to discrete membrane domains at cell-cell contacts. *Celsr1*- or *Vangl2*-deficient mice show valve aplasia due to failure of endothelial cells to undergo rearrangements and adopt perpendicular orientation at valve initiation sites. Mechanistically, we show that Celsr1 regulates dynamic cell movements by inhibiting stabilization of VE-cadherin and maturation of adherens junctions. These findings reveal a role for PCP signaling in regulating adherens junctions and directed cell rearrangements during vascular development.

INTRODUCTION

Tissue remodeling and formation of organs rely on cooperative behavior of cells in groups or layers and integration of inputs from neighboring tissues, which generate forces to drive morphogenic movements. Cell-cell junctions have emerged as key signal integrators that can sense and transduce mechanical tension and thus coordinate cell behaviors (Gomez et al., 2011). During morphogenesis, the junctions are dynamically remodeled to allow cells to move relative to each other but without losing their contact. For example, intercalation of cells during gastrulation, a process that drives anterior-posterior elongation of the body axis, relies on polarized remodeling of adherens junctions (AJs) to enable expansion of cell-cell adhesions in one plane of the epithelium and contraction in the perpendicular plane (Bertet et al., 2004).

The key components and regulators of cell-cell junctions are members of the cadherin family of cell-cell adhesion proteins, consisting of classical cadherins, protocadherins, and atypical cadherins (Fat, Dachsous, and Flamingo in *Drosophila*) (reviewed in Halbleib and Nelson, 2006). In addition to their role in mechanical cell-cell adhesion, cadherins participate in local regulation of the actin cytoskeleton and in diverse signaling pathways. Consequently, cadherins regulate a variety of developmental processes such as cell-cell recognition and sorting, coordination of morphogenic cell movements, and the establishment and maintenance of cell and tissue polarity (Halbleib and Nelson, 2006). A well-studied example of the last is the establishment of planar cell polarity (PCP) within an epithelial sheet (reviewed in Goodrich and Strutt, 2011; Gray et al., 2011; Seifert and Mlodzik, 2007) One of the core components of the PCP signaling pathway is the seven-pass transmembrane atypical cadherin Flamingo (Celsr1–3 in vertebrates), which orchestrates the establishment of polarized cell-cell junctions across proximodistal cell boundaries by recruiting an asymmetric complex consisting of Strabismus/Van Gogh-like (Vangl) and Frizzled to the membrane (Chen and Clandinin, 2008; Usui et al., 1999). The PCP pathway, first discovered in *Drosophila*, is a conserved regulator of epidermal planar polarity; disruption of PCP in vertebrates leads to defects in neural tube closure, stereocilia orientation of hair cells in inner ear and skin hair patterning (Curtin et al., 2003; Devenport and Fuchs, 2008; Kibar et al., 2001; Montcouquiol et al., 2003). However, it has recently been recognized that PCP signaling is utilized more widely to control polarized cell movements and tissue morphogenesis in a variety of organs. For example, core PCP genes regulate convergent-extension and polarized intercalation of mesenchymal cells during gastrulation (Carreira-Barbosa et al., 2009; Formstone and Mason, 2005; Tada and Smith, 2000; Wallingford et al., 2000) and of

neural progenitor cells across the midline into the contralateral neuroepithelial layer (Ciruna et al., 2006). PCP pathway is also implicated in the regulation of neuronal migration (Qu et al., 2010; Wada et al., 2006), dendrite growth (Gao et al., 2000; Matsubara et al., 2011), and target selection (Chen and Clandinin, 2008; Hakeda-Suzuki et al., 2011; Lee et al., 2003) as well as axon guidance and tract formation (Tissir et al., 2005; Zhou et al., 2008). PCP drives epithelial polarization by regulating actomyosin-dependent contraction of AJs (Nishimura et al., 2012), although it is less well understood how this pathway controls other processes that do not involve apparent planar polarization, such as neuronal migration.

Like other morphogenic processes, the development of the vascular system involves dynamic cell rearrangements and alterations in cell-cell contacts between individual endothelial cells, as has been observed in actively growing vascular sprouts and anastomosing vessels (Blum et al., 2008; Jakobsson et al., 2010). In addition, in the developing lymphatic and venous valves, endothelial cells undergo profound changes in their shape, polarity, and arrangement as part of a complex morphogenic process leading to the formation of two intraluminal leaflets (Bazigou et al., 2009, 2011; Sabine et al., 2012). However, the mechanisms that regulate endothelial cell-cell adhesion dynamics during development in vivo, including in valve morphogenesis, are not well understood. We show that the core PCP proteins Celsr1 and Vangl2 regulate directed cell rearrangements during lymphatic valve formation by controlling the stabilization of endothelial AJs.

RESULTS

Lymphatic Endothelial Cells Undergo Reorientation and Collective Migration into the Vessel Lumen to Initiate Valve Leaflet Formation

The earliest known sign of lymphatic valve formation is the appearance and clustering of cells expressing elevated levels of Prox1 and Foxc2 transcription factors in defined areas of the vessel (Bazigou et al., 2009; Norrmén et al., 2009; Sabine et al., 2012). The Prox1^{high} valve-forming cells initially cluster along the wall of embryonic day (E)16.5 mesenteric vessels (Figure 1A) (Sabine et al., 2012). Notably, at this stage the Prox1^{high} cells showed highly elongated nuclei and aligned along the longitudinal axis of the vessel (Figure 1A). In contrast, when valve leaflet formation was initiated at E17.5, Prox1^{high} cells reoriented by 90° and aligned perpendicular to the flow direction (Figure 1B) (Bazigou et al., 2009).

To better understand the changes in shape and relative arrangement of valve-forming cells, we induced mosaic labeling of endothelial cells in the developing lymphatic vessels with a membrane-bound fluorescent marker. For this purpose, *Prox1-CreER^{T2}* mice (Bazigou et al., 2011) were crossed with *R26-mTmG* reporter (Muzumdar et al., 2007). After administering the mice with a low dose of 4-hydroxytamoxifen (4-OHT), individual endothelial cells were visualized by GFP fluorescence (Figures 1C–1F′). Cell shape analysis, combined with visualization of the morphology and orientation of cell nuclei by Prox1 immunostaining, confirmed that the valve-forming cells adopted an elongated morphology at an early stage of valve formation and prior to cell reorientation (Figures 1C–1D′; Figures S1A–S1C available online). Cells that underwent reorientation maintained highly elongated morphology compared to those on the vessel wall (Figures 1E–1F′). During the reorientation process, the valve-forming cells also extended polarized membrane protrusions, indicative of active cell migration (Figures 1F and 1F′).

We further studied the developing valves using correlative fluorescence and transmission electron microscopy (TEM). Ring-shaped valves composed of reoriented endothelial cells were localized under a fluorescence microscope in the mesenteric lymphatic vessels of *Prox1-CreER^{T2};R26-mTmG* embryos (Figure 1G). Three-dimensional reconstruction of a vessel from serial images of semi-thin sections showed that the reoriented valve-forming cells protruded into the vessel lumen to form a disc-like structure (Figure 1H). Further analysis of cross sections of the disc revealed that they were composed of two or even multiple layers of endothelial cells that were in contact with each other but with no apparent extracellular matrix in between them (Figures 1I and 1J). TEM revealed discontinuous and low density cell-cell junctions between the valve-forming cells, suggesting dynamic regulation and high turnover of the junctions (Figures 1K, 1L, and 1L′). Such arrangement was unique to the early stage of valve formation. In mature lymphatic valve leaflets of postnatal mesenteric vessels continuous and high density overlapping junctions were observed between endothelial cells that were organized into two sheets separated by an extracellular matrix core (Figures 1M and 1M′) (Bazigou et al., 2009).

In summary, these results show that prior to the initiation of valve leaflet formation, the Prox1^{high} endothelial cells undergo dramatic cell shape and polarity changes, characterized by elongation and reorientation by 90°. This leads to the alignment of valve-forming cells perpendicular to the longitudinal axis of the vessel and is followed up by their collective migration into the vessel lumen. The organization of cell-cell junctions further suggests dynamic re-arrangements of valve-forming endothelial cells during this process.

Planar Cell Polarity Proteins Celsr1-3 and Vangl2 Are Expressed in Lymphatic Endothelial Cells of Luminal Valves

Planar cell polarity (PCP) pathway controls cell morphology, polarized cell movements, and tissue morphogenesis (Goodrich and Strutt, 2011; Gray et al., 2011; Seifert and Mlodzik, 2007). To address whether this pathway also regulates morphology and rearrangements of cells during valve morphogenesis, we first analyzed the expression of the core PCP protein Celsr1 in the developing vasculature. Celsr1 was not present in embryonic mesenteric lymphatic vessels before E16 (data not shown), however, its expression was induced at E16.5 upon valve initiation in areas of Prox1^{high} cell clusters (Figure 2A). Prominent Celsr1 expression was subsequently found in endothelial cells that reoriented perpendicular to the flow direction at E17.5, whereas punctuate staining remained in cells in the proximity of the constriction zone (Figure 2B). In E18.5 and postnatal mesenteric lymphatic vessels Celsr1 was largely restricted to the valve leaflets (Figures 2C and S2A). Celsr1 interactor Vangl2 colocalized with Celsr1 in the developing and mature valves (Figures 2D and S2A). In contrast, Frizzled 6, another key component of

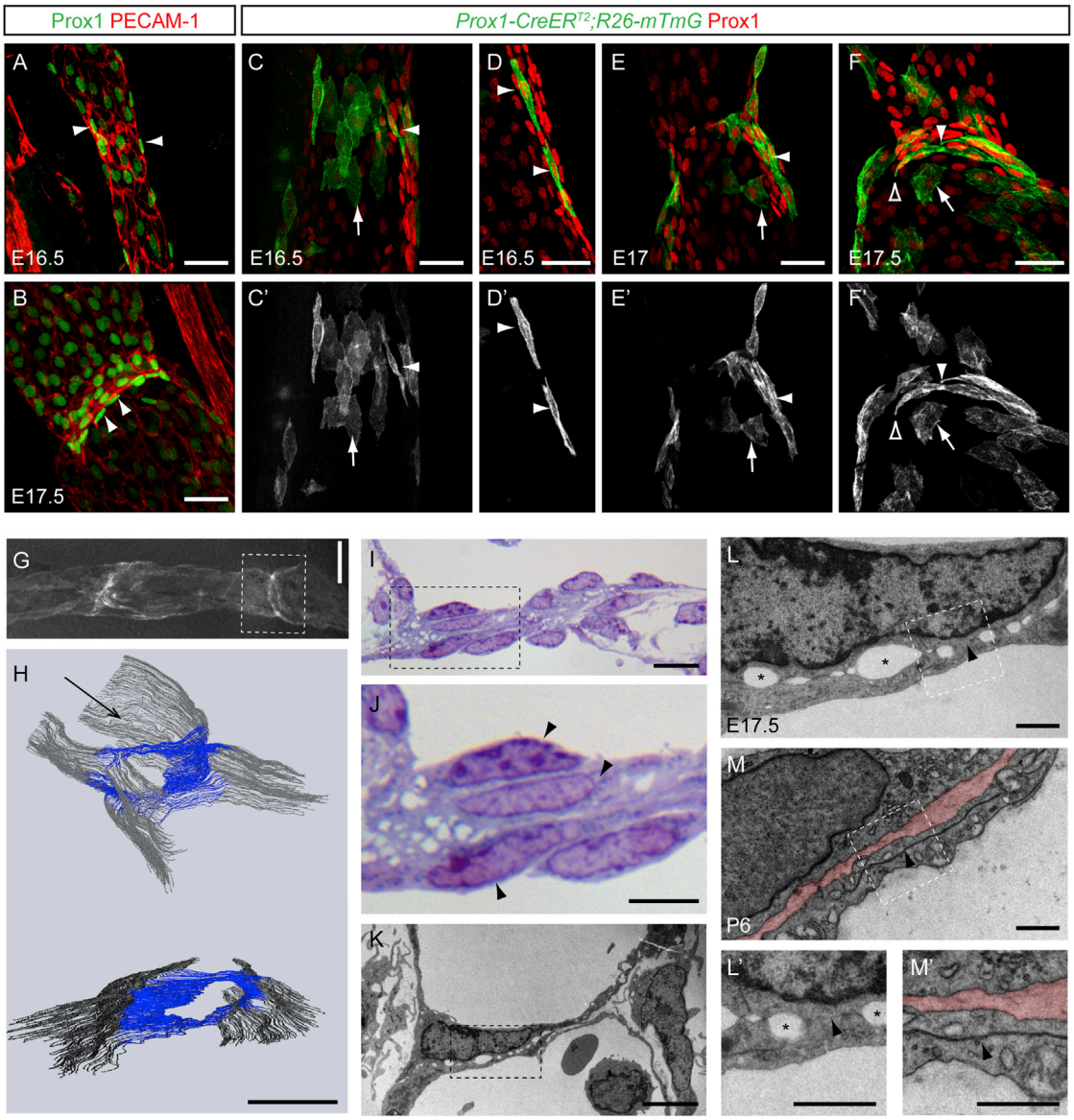

Figure 1. Lymphatic Endothelial Cells Elongate, Reorient by 90°, and Migrate Collectively to Vessel Lumen to Initiate Valve Leaflet Formation

(A and B) Whole-mount immunofluorescence of E16.5 (A) and E17.5 (B) wild-type mesenteric vessels for Prox1 (green) and PECAM-1 (red). Note the elongation of Prox1^{high} cells at E16.5 (arrowheads in A) and their reorientation by 90° at E17.5 (arrowheads in B).

(C–F′) Labeling of individual lymphatic endothelial cells with a membrane targeted GFP in *Prox1-CreER^{T2};R26-mTmG* mesentery. At all stages analyzed (E16.5–E17.5), Prox1^{high} valve forming cells show elongated shape (arrowheads) compared to cells on the vessel wall (arrows). Note polarized membrane protrusions in reorienting cells (open arrowhead in F and F′).

(G and H) Visualization of a "ring-shaped" valve in E17.5 mesenteric lymphatic vessel of *Prox1-CreER^{T2};R26-mTmG* reporter mouse (G). The boxed area shows a valve that was analyzed by serial sectioning for light microscopy and 3D reconstruction (H, shown at two different angles). Arrow in (H) shows the direction of flow. Blue color highlights valve endothelial cells forming a disc and gray represents the vessel wall.

(I and J) Semi-thin section stained with 1% toluidine blue showing a cross section of a valve "disc" in E17.5 mesentery. Boxed area in (I) is magnified in (J). Endothelial cells are present in multiple layers (arrowheads in J).

(K–M′) Transmission electron microscopy of developing (E17.5; K, L, and L′) and mature (P6; M and M′) valves in mesenteric lymphatic vessels. Boxed area in (K) is magnified in (L), and the areas in (L) and (M) are magnified in (L′) and (M′), respectively. Note discontinuous cell-cell junctions (arrowheads in L and L′) and large intercellular gaps (asterisks in L and L′) at E17.5, compared to continuous overlapping cell-cell junctions in mature valves (arrowhead in M and M′). Extracellular matrix core of the valve leaflet is highlighted in red in (M) and (M′).

Scale bars represent 40 μm (A–F), 100 μm (G and H), 10 μm (I), 5 μm (J and K), and 1 μm (L–M′).

See also Figure S1 and Movie S1.

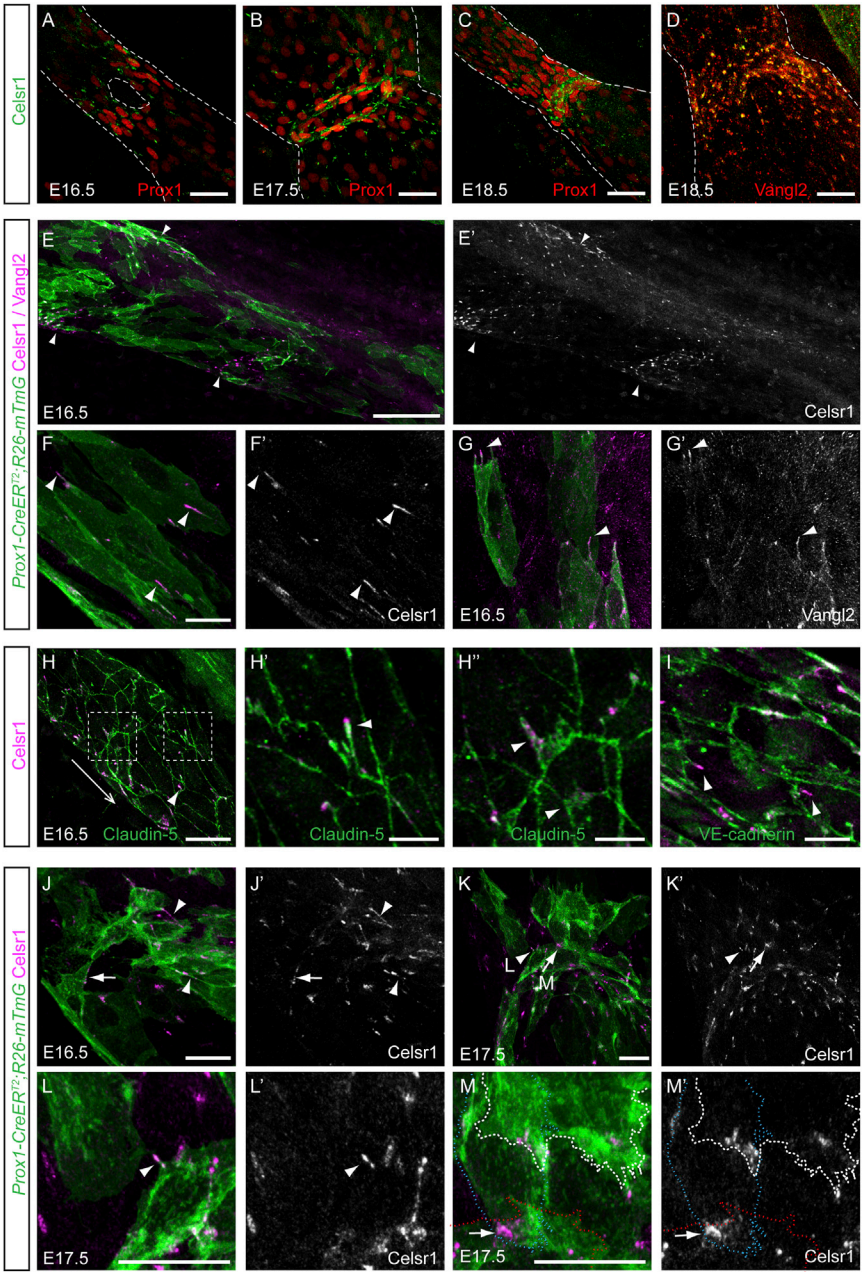

Figure 2. Core Planar Cell Polarity Proteins, Celsr1 and Vangl2, Are Recruited from Membrane Filopodia to Cell-Cell Contacts in the Valve-Forming Endothelial Cells

(A–C) Whole-mount immunofluorescence for Celsr1 (green) and Prox1 (red) at indicated stages of development. Note punctuate Celsr1 staining in areas of Prox1^{high} valve-forming cells. Dotted lines outline lymphatic vessels.

(D) Localization of Celsr1 (green) and Vangl2 (red) in mature valves.

(E–G′) Visualization of Celsr1 (purple, E and F) or Vangl2 (purple, G) in individually labeled lymphatic endothelial cells (marked by mGFP fluorescence (green) in *Prox1-CreER^{T2};R26-mTmG* vessels) at E16.5. (E and E′) Tile scan of E16.5 lymphatic vessel showing Celsr1 at areas of developing valves (arrowheads). (F–G′) Higher magnification images of vessels showing localization of Celsr1 (F and F′) and Vangl2 (G and G′) to the tips of membrane filopodia (arrowheads) at an early stage of valve development.

(H–I) Whole-mount immunofluorescence of E16.5 wild-type mesenteric lymphatic vessel for Celsr1 (purple), Claudin-5 (green, H–H″), or VE-cadherin (green, I). Boxed areas in (H) are magnified in (H′) and (H″). The direction of flow is indicated by an arrow. Note the localization of Celsr1 to the tips of Claudin-5+ and VE-cadherin+ filopodia (arrow in H′ and I) and membrane protrusions (H″).

(J–M′) Visualization of Celsr1 (purple) in individually labeled lymphatic endothelial cells (green) at indicated stages. Celsr1 is localized to cell-cell contacts (arrowheads in J–M′) and junctions (arrows in J–M′) in reorienting cells. (L and M) Magnifications of areas shown by arrowhead and arrow, respectively, in (K). Dotted lines in (M) and (M′) outline individual endothelial cells. Single channel images for indicated stainings are shown.

Scale bars represent 40 μm (A–D), 100 μm (E–E″), 40 μm (F–G′ and J–M′), 30 μm (H), 7.5 μm (H′ and H″), and 20 μm (I).

See also Figure S2.

the PCP signaling pathway, was expressed in lymphatic vessels but did not localize specifically to the valve regions (Figure S2B).

Celsr1 Is Recruited from Membrane Protrusions to Cell-Cell Contacts during Cell Reorientation

Next we studied the subcellular localization of Celsr1 by performing immunostaining on *Prox1-CreER^{T2};R26-mTmG* reporter mice in which mosaic labeling of individual cells was induced by a suboptimal dose of 4-OHT. Tile scan images of mesenteric lymphatic vessels along their entire length confirmed that Celsr1 expression was predominantly found at areas of developing valves (Figures 2E and 2E′). At E16.5, Celsr1 localized to the tips of membrane protrusions and filopodia (Figures 2F, 2F′ and S2C). Vangl2 was also recruited to filopodia, suggesting the presence of PCP signaling (Figures 2G and 2G′). Celsr1-enriched filopodia also expressed junctional proteins Claudin-5 (Figures 2H–2H″) and VE-cadherin (Figure 2I). Celsr1-positive filopodia oriented along the vessel with the majority pointing against the flow direction (Figure S2D), which suggests a possible role in sensing flow or directional cues. Celsr1 was also present in larger Claudin-5 positive protrusions of overlapping cells (Figure 2H″).

When cells reoriented, Celsr1 localized to the sites of filopodial contacts and along cell-cell junctions (Figures 2J–2M′). Interestingly, Celsr1 showed discontinuous and punctuate localization at the cell membrane both in developing (Figures 2J–2M′) and mature valves (Figure 2D). These expression data demonstrate that the reorientation of valve-forming cells coincides with the recruitment of Celsr1 from specialized tips of membrane filopodia to cell-cell contacts.

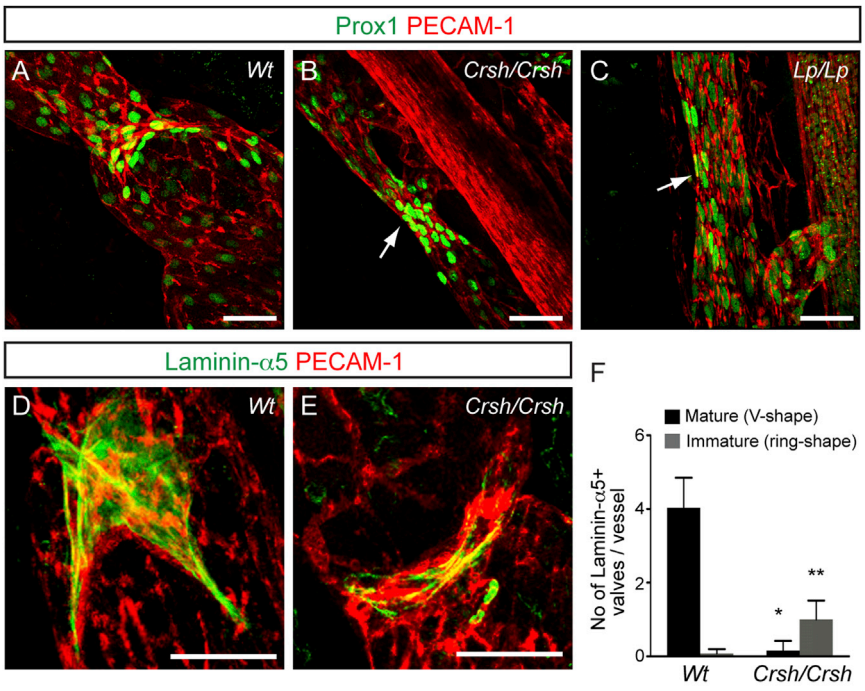

Figure 3. PCP Mutants Show Defect in Lymphatic Valve Morphogenesis

(A–C) Whole-mount immunofluorescence of E18.5 wild-type (A), *Crsh* (Celsr1 mutant; B), and *Looptail* (Vangl2 mutant; C) mesenteric lymphatic vessels for Prox1 (green) and PECAM-1 (red). Note abnormal valves in the mutants (arrows in B and C).

(D and E) Visualization of lymphatic valve leaflets in E18.5 in wild-type (D) and *Crsh* mutants (E) by Laminin-α5 (green) and PECAM-1 (red) staining.

(F) Quantification of Laminin-α5 positive valves in mesenteric lymphatic vessels. Mature valves (black bars) were defined as V-shaped and immature valves (gray bars) as ring-shaped structures (as in E). Data represent mean ± SD ($n \geq 5$). *$p < 0.0001$ and **$p < 0.001$ (Student's t test). Scale bars represent 40 μm (A–E).

PCP Signaling Is Required for Lymphatic Valve Morphogenesis

To study the role of PCP signaling in vivo in lymphatic valve formation, we analyzed mouse mutants *Crsh* and *Looptail*, which harbor point mutations in genes encoding *Celsr1* and *Vangl2*, respectively (Curtin et al., 2003; Kibar et al., 2001). Mesenteric lymphatic vessels of E18.5 embryos were stained for Prox1, to visualize lymphatic valves and the orientation of valve-forming cells, and for Laminin-α5, to highlight the matrix core of the valve leaflet (Bazigou et al., 2009). At this stage, the wild-type vessels showed mature valves with elongated Prox1^{high} cells and fully developed Laminin-α5 positive leaflets (Figures 3A and 3D). In *Crsh* and *Looptail* mutants, the valves were identified as clusters of Prox1^{high} cells that showed abnormal organization (Figures 3B and 3C). In addition, a reduced number of valves that were positive for Laminin-α5 were observed, and they failed to develop leaflets (Figures 3E and 3F). These results demonstrate a critical role for the core PCP proteins Celsr1 and Vangl2 in lymphatic valve morphogenesis.

Celsr1 Functions Tissue-Autonomously in Lymphatic Endothelia to Regulate Valve Formation

To further explore the role of PCP signaling in valve development, we generated a conditional deletion of *Celsr1* specifically in lymphatic endothelial cells using the *Prox1-CreER^{T2}* mice. Efficient depletion of Celsr1 protein was observed (Figures S3A–S3D″). Similar to the *Crsh* mutants, *Celsr1$^{flox/flox}$;Prox1-CreER^{T2}* (hereafter denoted as *Celsr1$^{-/-}$*) embryos showed abnormal lymphatic valves compared to the controls at E18.5 (Figures 4A and 4B). The defect was specific to Celsr1 function because normal valves were observed in *Celsr2$^{-/-}$* and *Celsr3$^{flox/flox}$;Prox1CreER^{T2}* (hereafter denoted as *Celsr3$^{-/-}$*) mice (Figures S3E and S3F). Interestingly, however, a more severe defect in valve formation was observed in embryos that lacked both *Celsr1* and *Celsr3* (Figures 4E and S3G), suggesting that Celsr3 can functionally compensate for Celsr1. Consistent with the previously demonstrated role of Celsr1 in recruiting Vangl2 to the cell membrane (Bastock and Strutt, 2007; Devenport and Fuchs, 2008; Strutt, 2001), Vangl2 was absent in *Celsr1$^{-/-}$* vessels (Figures 4C and 4D).

Quantification revealed that the total number or valves was similar in *Celsr1$^{-/-}$* (32.3 ± 7.65, n = 10) and *Celsr1$^{-/-}$;Celsr3$^{-/-}$* (28 ± 3.54, n = 5) vessels compared to the control (34.7 ± 6.5, n = 7) at E18.5 (Figure 4E). However, a significantly larger proportion of mutant valves were immature or abnormal. Immature valves, which were also detected at lower frequency in control vessels at E18.5, showed reorientation of Prox1^{high} cells but no leaflets ("ring-shape", Figures 4E and S3B). The majority of mutant valves were characterized by Prox1^{high} cells remaining aligned parallel to the vessel axis (Figures 4B and S3C) or showing random orientation (Figure S3D). Although both Celsr1 and Vangl2 continued to be expressed in fully developed valves (Figure S2A), deletion of *Celsr1* and *Celsr3* in the mature lymphatic vessels of 3-week-old mice did not lead to valve defects (Figures 4F and 4G). Together, these in vivo data demonstrate a specific role for PCP signaling in regulating cell reorientation during valve morphogenesis, although it is not required for determining the sites of developing valves or valve maintenance.

Celsr1 Deficiency Leads to Defects in the Organization of Endothelial Junctions and Cell Reorientation during Valve Formation

Given the ability of Celsr1 to mediate homophilic adhesion, we next analyzed endothelial cell junctions in the control and mutant vessels by Claudin-5 staining. Lymphatic endothelial cells of control vessels formed continuous "zipper-like" junctions, except for the cells forming the valves, which had less defined junctions with junctional discontinuities (Figures 4H and 4H′). In contrast, cell-cell junctions of *Celsr1$^{-/-}$;Celsr3$^{-/-}$* vessels were disorganized. They showed large protrusions and uneven distribution of Claudin-5 along the junctions (Figures 4I and 4I′).

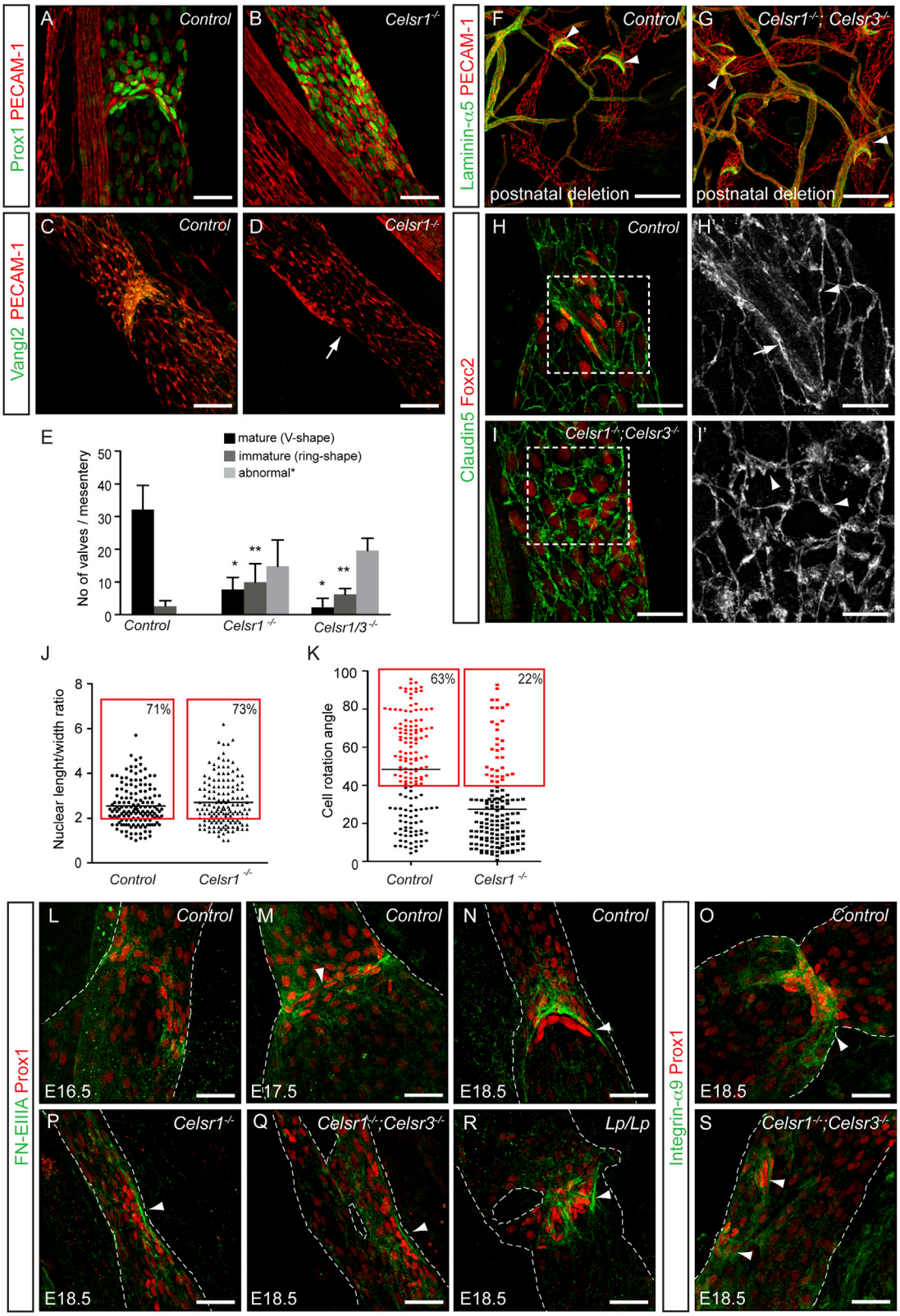

Figure 4. Celsr1 Is Required for Lymphatic Endothelial Cell Reorientation during Valve Formation

(A–D) Whole-mount immunofluorescence of E18.5 mesenteric lymphatic vessels for Prox1 (green, A and B) or Vangl2 (green, C and D) and PECAM-1 (red). Note the lack of Vangl2 in *Celsr1* deficient vessel (arrow in D).

(legend continued on next page)

In order to further decipher the function of Celsr1 in vivo, we analyzed the valves at an earlier stage at E17.5, when most Prox1^{high} cells in control vessels aligned perpendicular to the flow direction but valve leaflets were not yet formed (Figures S3H, S3H′, and 1B). At this stage, *Celsr1*$^{-/-}$ valves contained a similar number of Prox1^{high} cells compared to control (Figure S3I and data not shown). Furthermore, the same proportion of valve-forming cells in mutant and control vessels displayed elongated morphology with a nuclear length/width ratio greater than two (Figure 4J). However, assessment of cell orientation by measuring the rotation angles of Prox1^{high} cells in respect to the longitudinal axis of the vessel (Figure S3I) showed that only 22% of mutant compared to 63% of control cells were in the process of reorienting perpendicular to the vessel wall (Figure 4K). Instead, the majority of the mutant Prox1^{high} cells remained aligned parallel to the vessel axis showing <40° angle of rotation (Figure 4K).

Celsr1-Regulated Cell Reorientation Is an Active Cellular Process that Precedes Assembly of FN-EIIIA+ Valve Matrix into a Perpendicular Ring Structure

Valve leaflets contain an extracellular matrix core composed of Laminin-α5 and Fibronectin containing the alternatively spliced EIIIA/EDA domain (FN-EIIIA) (Bazigou et al., 2009). Alignment of Prox1^{high} cells perpendicular to the flow direction coincides with upregulation of the FN-EIIIA receptor, Integrin-α9, and the organization of FN-EIIIA into a ring structure at the sites of developing valves (Figures 4L and 4M) (Bazigou et al., 2009). In mature valves, Integrin-α9 and FN-EIIIA are subsequently found on valve endothelial cells or the free edges of the leaflets, respectively (Figures 4N and 4O) (Bazigou et al., 2009). Fibronectin matrix assembly, which can also be regulated by Cadherin activity (Dzamba et al., 2009), could, therefore, indirectly regulate cell reorientation during valve formation. Despite abnormal orientation of Prox1^{high} cells, *Celsr1*$^{-/-}$ and *Celsr1*$^{-/-}$;*Celsr3*$^{-/-}$ valves showed normal deposition of FN-EIIIA (Figures 4P and 4Q). Prominent FN-EIIIA fibers were also observed in valve areas in *Looptail* mutant vessels, even in those that displayed random orientation of Prox1^{high} cells (Figure 4R). Consistent with its requirement for FN-EIIIA assembly (Bazigou et al., 2009), Integrin-α9 was present in *Celsr1*$^{-/-}$;*Celsr3*$^{-/-}$-deficient valves (Figure 4S).

Together, these results show that the failure of PCP mutant valve-forming endothelial cells to adopt correct orientation is not due to defective assembly of extracellular matrix. Instead, they indicate that cell reorientation is an active Celsr1-regulated process that precedes matrix assembly.

Lymphatic Endothelial AJs Undergo Maturation from Overlapping Membrane Contacts to Linear Junctions In Vitro

To understand the cell-cell junction defects in the PCP mutant mice, we studied primary lymphatic endothelial cells (LECs) at different confluence states, which are known to regulate the organization of AJs. Analysis of the changes in junction morphology during different stages of cell-cell contact formation and stabilization revealed a junction maturation process in the LECs. When plated at low confluence, within 24 hr LECs formed "islands" in which the cells established stable contacts with each other, rather than migrating as single cells (data not shown). Under these conditions the majority of their junctions were characterized by the presence of large overlapping membrane protrusion in between the neighboring cells (Figures S4A and S4C). The number of overlapping junctions, as well the width of the junctional structures, decreased over time when the cells reached confluence and the junctions acquired a linear morphology (Figures S4A and S4B). During their stabilization, there was a gradual enrichment of VE-cadherin at the junctions (Figure S4C). Confluent LECs displayed cortical actin when VE-cadherin was stabilized at the mature junctions, whereas under the same conditions, the blood endothelial cells showed stress fibers and mainly overlapping junctions (Figure S4D) (Petrova et al., 2002).

Celsr1 Localizes to Specific Membrane Domains at Endothelial Cell Junctions

To study the potential role of Celsr1 in regulating cell-cell junctions, we examined its localization and function in the primary LECs that were transfected with Celsr1-GFP and analyzed at different confluence states. Like in epithelial cells (Devenport and Fuchs, 2008), Celsr1-GFP was diffuse in isolated LECs (data not shown). Upon contact between two transfected cells, Celsr1-GFP was rapidly recruited to the sites of contact (Movie S2). Under subconfluent conditions Celsr1 localized to

(E) Quantification of valve morphology (based on Prox1/PECAM-1 staining) in the mutant mice at E18.5. Three different categories were defined: mature (V-shape; black bars), immature (ring-shape; dark gray bars) and abnormal (no reorientation or misalignment of Prox1^{high} cells; light gray bars). Data represent mean ± SD ($n \geq 5$). *$p < 0.0001$, **$p < 0.01$, compared to control (Student's t test).
(F and G) Whole-mount immunofluorescence of adult ears, following postnatal deletion of *Celsr1*/*Celsr3*, for Laminin-α5 (green) and PECAM-1 (red). Normal valves are observed in the mutant when compared to the control (arrowheads in F and G).
(H–I′) Visualization of cell junctions using Claudin-5 staining at E18.5. Note zipper-like junctions in the control (arrowhead in H′), except between valve-forming cells (arrow in H′) and disorganization of junctions in the mutant vessel (arrowheads in I′).
(J) Analysis of the shape of Prox1^{high} cell nuclei in E17.5 mesenteric vessels ($n \geq 9$). Individual values are plotted. Black line indicates mean. The proportion of cells (%) showing elongated morphology with nuclear length/width ratio >2 (gray dotted line) is shown.
(K) Orientation of Prox1^{high} cells in E17.5 mesenteric vessels. Individual values showing rotation angles of Prox1^{high} cells with respect to the longitudinal axis of the vessel are plotted. 0° = longitudinal, 90° = perpendicular alignment to the axis of the vessel. Black line indicates mean. Reoriented cells that showed >40° angle (gray dotted line) are shown in red and their proportion (%) is indicated. $p < 0.0001$ (Mann-Whitney test).
(L–S) Whole-mount immunofluorescence of wild-type (L-N), *Celsr1*$^{-/-}$ (P), *Celsr1*$^{-/-}$;*Celsr3*$^{-/-}$ (Q and S), and *Looptail* (R) mesenteric lymphatic vessels at indicated stages for Prox1 (red) and FN-EIIIA (green) or Integrin-α9 (green). FN-EIIIA organizes into fibers (arrowheads in M and N) when Prox1^{high} cells reorient. Note the assembly of FN-EIIIA fibers and the presence of Integrin-α9 in the valve areas in mutant vessels (arrowheads in O–S). Dotted lines outline lymphatic vessels.
Scale bars represent 40 μm (A–D and L–S), 100 μm (F and G), 30 μm (H and I), and 15 μm (H′ and I′),
See also Figure S3.

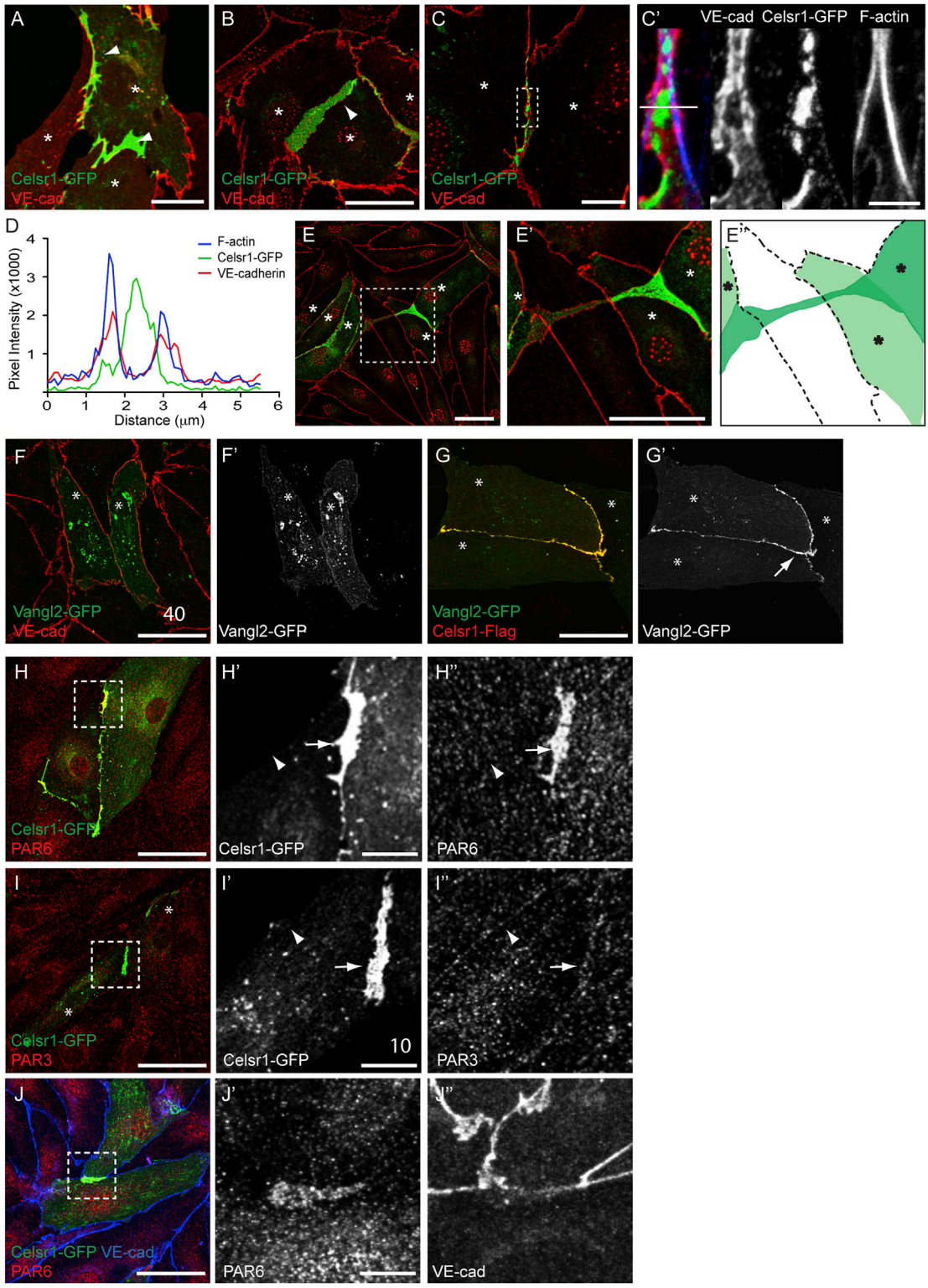

Figure 5. Celsr1 Localizes to Specific Membrane Domains within Cellular Protrusions in Primary Lymphatic Endothelial Cells

(A–E′) Celsr1-GFP (green) and VE-cadherin (red) localization during the establishment (A and B) and maturation (C) of cell-cell junctions. Note mutually exclusive localization of Celsr1-GFP and VE-cadherin/F-actin to specific membrane domains (C′). Single channel images for Celsr1-GFP, VE-Cadherin, and F-actin are included as indicated. (E and E′) show a Celsr1-GFP positive cell making contact to a distant Celsr1 positive cell underneath another cell. (E″) shows schematic representation of cell arrangement. Asterisks indicate cells expressing Celsr1-GFP. (D) Intensity scan profile showing pixel intensity values for Celsr1-GFP (green), VE-cadherin (red), and F-actin (blue) measured across a cell-cell junction. The position of the scan line is shown in (C′).

(legend continued on next page)

membrane protrusions in between cells and to filopodia originating from the protrusions that were highly dynamic (Figures 5A, 5B, S5A and S5B; Movie S2). Celsr1 did not induce the formation of these filopodia as they were also observed in control cells expressing membrane-bound YFP (Movie S3). Interestingly, Celsr1 positive membrane protrusions sometimes extended underneath other cells (Figures 5E–5E″; Movie S4) and formed a connection with a distant Celsr1 expressing cell (Figures 5E–5E‴). However, Celsr1 did not mediate stable adhesion because cells were able to migrate away from each other after forming contacts (Movie S4).

In confluent LECs, Celsr1 showed a punctuate pattern along the junctions (Figure 5C). However, in contrast to epithelial cells where Celsr1 localized to E-cadherin containing AJs (Nishimura et al., 2012), in the LECs, Celsr1-GFP showed a mutually exclusive localization with VE-cadherin and F-actin to discrete membrane domains (Figures 5C′ and 5D). Celsr1-GFP also did not colocalize with the components of tight junctions, including Claudin-5 and ZO-1 (Figure S6). Furthermore, Myosin IIB and phosphorylated myosin light chain (pMLC), which is the active form of Myosin II implicated in PCP-mediated contraction of epithelial AJs (Nishimura et al., 2012), did not colocalize with Celsr1 (Figure S6). In contrast, Vangl2 was specifically recruited to cell junctions with Celsr1 in a Celsr1-dependent manner (Figures 5F–5G′).

To further characterize the molecular composition of Celsr1-positive junctions, we analyzed the recruitment of the PAR complex (PAR6/PAR3/aPKC), which is known to regulate polarity in epithelial cells. Surprisingly, we found that PAR6 was recruited specifically to Celsr1 positive cell-cell junctions in the absence of PAR3 and aPKC (Figures 5H–5I″ and data not show). A distinct PAR3-PAR6 complex that lacks aPKC was previously demonstrated in blood endothelial cells (Iden et al., 2006). This complex was shown to localize to adherens junctions by binding to VE-cadherin (Iden et al., 2006). However, in the LECs PAR6 was found at the Celsr1 positive junctions prior to the recruitment of VE-cadherin (Figures 5J–5J″).

These results show a similar localization of Celsr1 at the endothelial membrane protrusions and cell-cell junctions in vitro as observed in vivo in the developing lymphatic valves. This localization and the molecular composition of the Celsr1 positive adhesive structures appear to be unique to lymphatic endothelial cells, because, in contrast to epithelial cells, they do not contain other classical junctional proteins but instead recruit the polarity proteins Vangl2 and PAR6.

Celsr1 Inhibits Stabilization of Endothelial AJs by Delaying VE-Cadherin Recruitment

Next we asked whether the presence of Celsr1 has functional consequences on junctional organization in the LECs. We first compared the localization of Celsr1-GFP and VE-cadherin-GFP in subconfluent LECs with PECAM-1 immunostaining. As described above, Celsr1-GFP localized predominantly to immature junctions displaying large membrane protrusions (Figures 6A–6A″ and 6C). In contrast, VE-cadherin-GFP showed an exclusive localization to mature cell-cell junctions, whereas the majority of the VE-cadherin-GFP negative junctions showed overlapping membrane contacts under these conditions (Figures 6B–6B′). The ability of the overexpressed VE-cadherin to induce mature junctions in the LECs is in agreement with previous studies using blood endothelial cells, which have established a key role for VE-cadherin in controlling the stability and maturation of AJs. In contrast to the overexpressed protein, endogenous VE-cadherin localized to membrane protrusions in subconfluent LECs. However, in the presence of Celsr1 VE-cadherin levels at the junctions were reduced (Figures 6D–6G). The C-terminal domain of Celsr1 was not required for VE-cadherin regulation (Figures 6H and 6H′).

To test if VE-cadherin regulation by Celsr1 was mediated via increased internalization, cells were treated with chloroquine, which inhibits protein degradation and recycling to the membrane and thus allows the visualization of internalized VE-cadherin. The level of VE-cadherin internalization in the LECs was low, and this was not affected by the presence of Celsr1 at the cell-cell contacts (Figure S7). Next we addressed the possibility that Celsr1 affects the initial recruitment of VE-cadherin to the junctions. After transfection, LECs were cultured in the presence of EGTA to inhibit calcium-dependent junction formation until Celsr1-GFP expression was detected (Figures 6I and 6I′). Following the removal of EGTA, synchronized formation of junctions that were positive for VE-cadherin was observed (Figures 6J and 6J′). However, Celsr1-positive contacts lacked VE-cadherin (Figures 6J and 6J′).

Our data demonstrate that Celsr1 does not disrupt established VE-cadherin positive junctions in vitro and is not required for their maintenance in vivo (see Figure 4G). Instead, the recruitment of Celsr1 to newly established immature junctions leads to a delay in the recruitment of VE-cadherin, thereby inhibiting the formation of stabilized AJs. Together, our data show a specific requirement for PCP signaling in directing rearrangements of valve-forming endothelial cells through regulation of endothelial AJ formation and stabilization (Figure 7).

DISCUSSION

Dysfunction of intraluminal valves interferes with the ability of the lymphatic system to collect and drain protein-rich fluid from the tissues, which can result in swelling called lymphedema (Alitalo, 2011). In this study, we describe a morphogenic process that involves reorientation and collective migration of valve-forming endothelial cells as they initiate valve leaflet formation. We further demonstrate an unexpected function for the component

(F–G′) Localization of Vangl2-GFP (green) with endogenous VE-cadherin (red, F) or Celsr1-Flag (red, G). Note the recruitment of Vangl2-GFP to cell-cell contacts only in presence of Celsr1-Flag (arrow in G′).
(H–J″) PAR6 and PAR3 localization in Celsr1-GFP expressing cells. Single channel images of the boxed areas are shown. Note the specific recruitment of PAR6 to Celsr1 positive (arrow in H′ and H″) but not negative (arrowhead in H′ and H″) junctions whereas weak PAR3 signal is observed at both junctions (arrow and arrowhead in I′ and I″). PAR6 is recruited to Celsr1 positive junctions before the arrival of VE-cadherin (J–J″).
Scale bars represent 40 μm (A–C, E–G′, H, I, and J), 10 μm (C, H′, H″, I′, I″, J′, and J″), and 2.5 μm (C′).
See also Figures S4–S6 and Movies S2, S3, and S4.

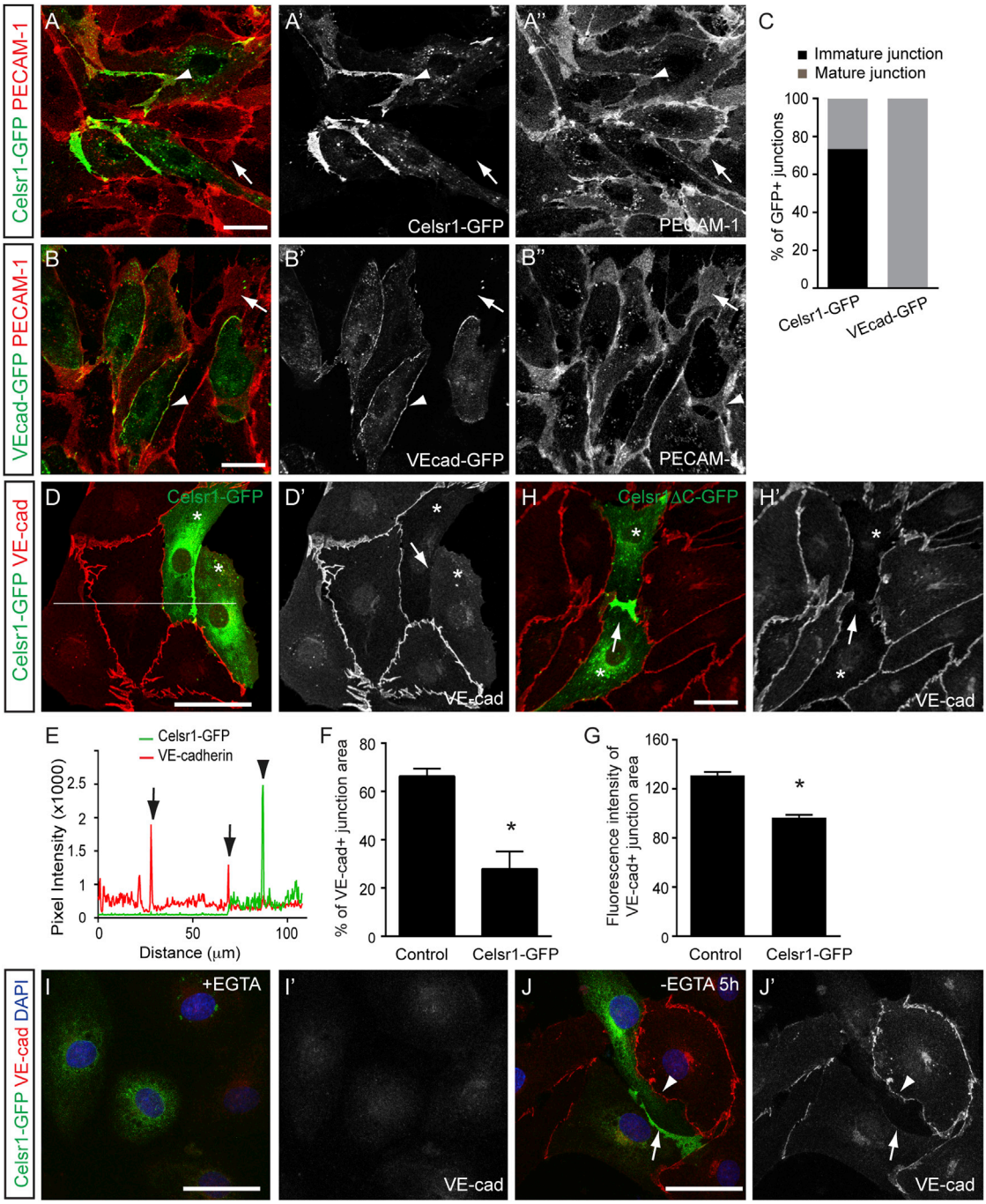

Figure 6. Celsr1 Regulates Lymphatic Endothelial Adherens Junctions

(A–B″) Localization of Celsr1-GFP (A, arrowhead) and VE-cadherin-GFP (B, arrowhead) in the LECs, costained for PECAM-1. Single channel images are shown on the right. Note the presence of membrane protrusions (arrows) except in the VE-cadherin-GFP-positive junctions.

(C) Quantification of VE-cadherin-GFP and Celsr1-GFP positive cell contacts (n = 174 junctions for Celsr1-GFP and n = 88 for VE-cad-GFP) showing protrusions (immature) or linear junctions (mature).

(D and D′) VE-cadherin immunostaining in Celsr1-GFP expressing cells. Note the reduction of VE-cadherin at the junction in between two Celsr1-GFP expressing cells (arrows) compared to control cells.

(E) Intensity scan profile showing pixel intensity values for Celsr1-GFP (green) and VE-cadherin (red) measured across cell junctions. The position of the scan line is shown in (D).

(F) VE-cadherin positive junction area measured at overlapping membrane contacts in control and Celsr1-GFP positive junctions. Data represent mean ± SEM (n = 3 experiments) *p < 0.0001 (Student's t test).

(G) VE-cadherin levels, measured as fluorescence intensity of VE-cadherin positive area, in control and Celsr1-GFP positive junctions. Data represent mean ± SEM (n = 63 junctions) of a representative experiment of three independent experiments *p < 0.0001 (Student's t test).

(legend continued on next page)

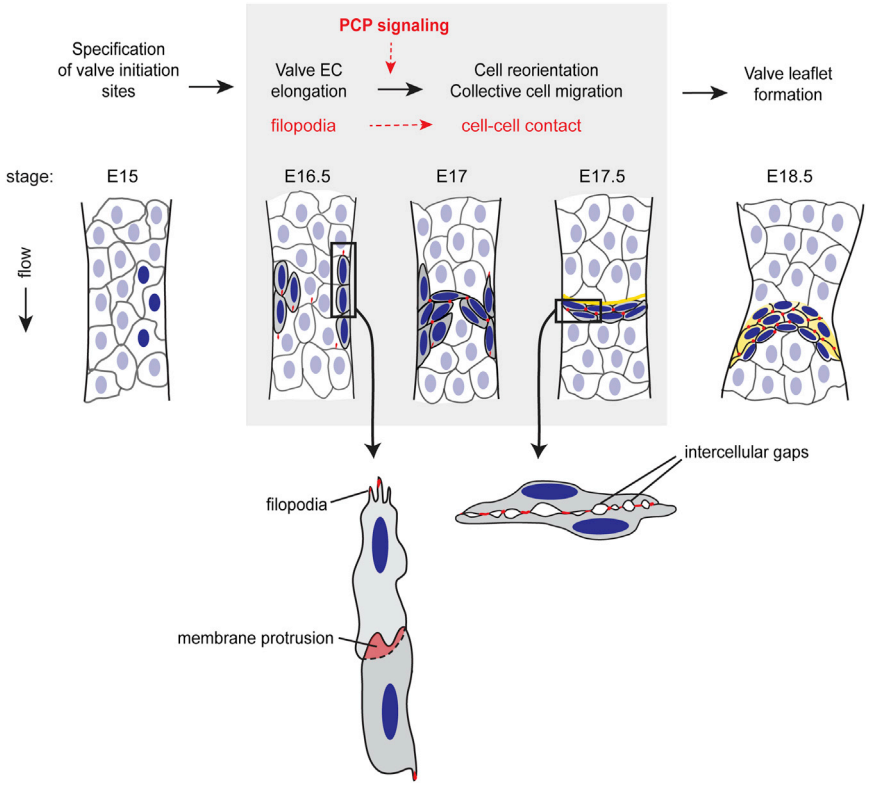

Figure 7. PCP Signaling in Lymphatic Valve Formation

Schematic model showing the elongation and reorientation of Prox1^{high} valve-forming cells (gray cells with dark blue nuclei) at early stages of valve formation and recruitment of Celsr1 (red) from endothelial filopodia and membrane protrusions to cell-cell contacts during this process. Yellow = extracellular matrix of the valve leaflet. Stages of development (E, embryonic day) are based on mouse mesenteric lymphatic vessels.

of the conserved PCP signaling pathway, Celsr1, in controlling endothelial AJ formation and directed cell rearrangements during valve formation.

Lymphatic valves develop through a complex morphogenetic process during which endothelial cells receive multiple signals from different sources, including those generated by flow-induced shear stress as well as cell-cell and cell-matrix communication (reviewed in Bazigou and Makinen, 2012). During valve initiation, endothelial cells at specific vessel locations acquire a unique identity. For example, valve-forming endothelial cells express elevated levels of Prox1 and Foxc2 transcription factors and activate Calcineurin/NFATc1 signaling (Norrmén et al., 2009; Sabine et al., 2012). It was recently shown that mechanosensory responses to shear stress, caused by the initiation of lymph flow, play an important role in inducing the valve endothelial cell phenotype (Sabine et al., 2012). In particular, acquisition of cuboidal cell shape was shown to be a hallmark of a lymphatic valve endothelial cell phenotype that was induced in cultured cells by cooperative function of Prox1 and oscillatory shear stress (Sabine et al., 2012). We show that in vivo, the Prox1^{high} valve-forming endothelial cells adopted a highly elongated, rather than cuboidal, morphology.

Our study further revealed a process of collective migration of endothelial cells as they initiate valve leaflet formation. The elongated Prox1^{high} cells first reorient by 90°, which resulted in their alignment perpendicular to the flow direction and the formation of transverse ridges on the vessel wall (Bazigou et al., 2009, 2011; and present study). These ridges subsequently extend into the vessel lumen to form a disc-like structure composed of multilayered endothelium displaying an organization of cell-cell junctions with multiple intercellular gaps. In contrast to mature valves, no apparent layer of extracellular matrix was detected in between cells of developing valve leaflets. These features are highly unexpected in view of our understanding of the organization of endothelium as a monolayer of endothelial cells that are firmly attached to each other and the underlying basement membrane. Interestingly, the collective cell migration properties of valve-forming endothelial cells during the cell reorientation process are reminiscent of mammary epithelial cells at the invading terminal end buds, which also show downregulation of adherens junctions, formation of intercellular gaps, and loose cell-cell contacts characterized by interdigitating membrane protrusions (Ewald et al., 2012).

The dynamic process of reorientation and collective migration of valve-forming cells is likely to require active remodeling of junctions to allow cells to move in respect to each other. We found that lymphatic valve formation required the core PCP proteins, Celsr1 and Vangl2, which have previously been implicated in regulating cell rearrangements and collective cell movements in other tissues (Bastock and Strutt, 2007; Carreira-Barbosa et al., 2009; Ciruna et al., 2006). Celsr1 function was specifically required for valve-endothelial cell reorientation; its deletion did not affect valve initiation, elongation of valve-forming endothelial cells, valve matrix assembly, or valve maintenance. Similar mechanisms were recently shown to control

(H and H′) VE-cadherin immunostaining in Celsr1ΔC-GFP expressing cells showing reduction of VE-cadherin at the Celsr1-positive junction (arrow) compared to control cells.

(I–J′) VE-cadherin (red) and DAPI (blue) staining in Celsr1-GFP (green) expressing cells in the presence (I) or 5 hr after the removal of EGTA (J). Note reduced VE-cadherin recruitment to a Celsr1 positive (arrow) when compared to a Celsr1 negative junction (arrowhead in J′).

Scales bars represent 40 μm.

See also Figure S7.

valve morphogenesis in lymphatic vessels and veins (Bazigou et al., 2011). However, our preliminary investigations have, for technical reasons due to difficulties in achieving efficient gene deletion in venous endothelia prior to valve initiation, failed to reveal a function for PCP signaling during venous valve formation (E. Bazigou and T.M., unpublished data). Efficiently targeted conditional approaches will be needed to address this question.

Celsr1 showed a subcellular localization pattern in lymphatic endothelial cells that is different from its localization to the apicolateral plasma membrane in epithelial cells. During early stages of valve development, Celsr1 and Vangl2 localized primarily to the tips of Claudin-5 and VE-cadherin-positive endothelial cell protrusions. Concomitant with the reorientation of the valve-forming endothelial cells Celsr1 was recruited to discrete membrane domains within cell-cell contacts, however, it showed a mutually exclusive localization with components of adherens/tight junctions and actomyosin. This is in contrast to epithelial cells where PCP core proteins were reported to localize to and regulate actomyosin-dependent contraction of AJs (Nishimura et al., 2012). Interestingly, however, analysis in *Drosophila* of the turnover rates of the PCP core proteins Fmi/Fz/Stbm (Celsr1/Frizzled/Vangl) revealed their presence in punctuate structures, representing stable asymmetric protein complexes that did not localize to epithelial AJs (Strutt et al., 2011).

Celsr1 also did not show an apparent planar polarized distribution in lymphatic endothelia, in contrast to its asymmetric localization along anterior-posterior sides of the epithelial cell plasma membrane (Devenport and Fuchs, 2008). It appears that the PCP complex, as we best understand it in polarized epithelium, has different composition and functions in nonepithelial tissues. For instance, Vangl2 is enriched in the filopodia of axon growth cones (Shafer et al., 2011) and mediates neuronal migration independent of Dishevelled, the key downstream component of the PCP pathway (Glasco et al., 2012), but through interaction with several non-PCP genes (Nambiar et al., 2007; Sittaramane et al., 2009). PCP signaling was also shown to control the formation of cellular protrusions and collective migration of *Drosophila* border cells during oogenesis (Bastock and Strutt, 2007). Interestingly, we found specific recruitment of PAR6 to Celsr1-positive lymphatic endothelial cell junctions. The lack of other components of the PAR polarity complex, PAR3/aPKC, and the lack of association of the Celsr1-positive junctions with actin or microtubules suggest that PAR6 may have an independent function in regulating AJs, different from its role in cell polarization (Bose and Wrana, 2006).

How does Celsr1 regulate the specific cellular processes that valve-forming endothelial cells undergo upon initiation of valve leaflet formation? Homophilic interaction between Celsr1 (Chen and Clandinin, 2008; Devenport and Fuchs, 2008; Usui et al., 1999) could increase the adhesive properties of Celsr1+/Prox1^{high} cells and thus enable the valve-forming cells to recognize, cluster, and maintain specific cell-cell contacts with each other. Consistent with homophilic binding, our in vitro analyses showed recruitment of Celsr1 to endothelial cell-cell contacts, however, they also showed lack of stable adhesion between Celsr1 expressing cells. Instead, we found that the rapid recruitment of Celsr1 to newly established cell-cell contacts delayed recruitment of VE-cadherin, the major adhesive component of the endothelial AJs. The recruitment and stability of VE-cadherin at the junctions is strictly regulated to maintain endothelial integrity and barrier function, but also to enable cell migration and vessel sprouting (Dejana and Giampietro, 2012; Gaengel et al., 2012). In particular, VE-cadherin flow at membrane protrusions was shown to facilitate the sliding of one cell underneath another contacting cell in order to promote active cell migration (Kametani and Takeichi, 2007). Although further studies are required to understand how Celsr1 regulates VE-cadherin, our in vivo and in vitro data indicate that this regulation provides an important mechanism that enables dynamic organization of junctions and rearrangements of cells during valve formation.

In summary, we show a specific requirement for the PCP proteins, Celsr1 and Vangl2, in controlling directed cell rearrangements during lymphatic valve formation. Celsr1-mediated VE-cadherin regulation further indicates an important role for PCP signaling in the control of endothelial adherens junctions, which may have implications for diverse PCP-regulated cellular processes in other tissues.

EXPERIMENTAL PROCEDURES

Mice

Mouse strains (*Prox1-CreER^{T2}*, *R26-mTmG*, *Celsr2$^{-/-}$* and conditional *Celsr1^{flox}* and *Celsr3^{flox}*; see Supplemental Experimental Procedures for details) were backcrossed to C57BL/6J for at least three generations. *Looptail* was analyzed on mixed Le/C57BL/6J background. *Crsh* mutant embryos (Curtin et al., 2003) were provided by Dr. J. Murdoch, MRC Harwell. The morning of vaginal plug detection was considered as embryonic stage E0. For gene deletion at embryonic stages, three consecutive intraperitoneal (i.p.) injections of 2 mg of 4-OHT, dissolved in peanut oil, were administered to pregnant *Celsr1/3;Prox1-CreER^{T2}* females at E15.5, E16.5, and E17.5 and the embryos were analyzed at E18.5. Mosaic GFP labeling of endothelial cells in *R26-mTmG;Prox1-CreER^{T2}* embryos was induced by a single i.p. injection of 0.5 mg of 4-OHT. Alternatively, 3-week-old mice were fed with tamoxifen containing diet (Harlan Teklad CRD TAM400) for 2 weeks. All mouse experiments were approved by the United Kingdom Home Office.

Cell Culture and Transfection

Human lymphatic endothelial cells (LEC) were obtained from PromoCell. Cells were seeded in Fibronectin-coated dishes with ECGMV2 medium (PromoCell) supplemented with 25 ng/ml of VEGF-C (R&D Systems). LEC were transfected by electroporation using Amaxa Nucleofector kit and protocol optimized for human umbilical vein endothelial cells with plasmids encoding Celsr1-GFP, Celsr1ΔC-GFP, Celsr1-Flag, Vangl2-GFP (Devenport and Fuchs, 2008), or VE-cadherin-GFP (cDNA encoding human VE-cadherin cloned into pEGFP-N1 vector [Clontech Biosciences]). For pEYFP-CAAX vector, the C-terminal CAAX domain of human K-Ras was cloned in pEYFP-N1. Subconfluent and confluent LECs monolayers were obtained by culturing cells on 24-well plates and Ibidi culture-inserts, respectively, and the cells were analyzed 24 hr after transfection.

Image Acquisition and Quantitative Analyses

Immunofluorescence staining was performed as previously described (Bazigou et al., 2009) (see Supplemental Experimental Procedures for details of antibodies). Confocal images of tissue whole-mounts were acquired using Zeiss LSM 510, 710, or 780 microscopes with Plan Apochromat DIC 40×/1.3 NA or Plan Apochromat DIC 63×/1.4 NA oil objective. All images represent maximum intensity projections of confocal z stacks that were generated using Imaris Bitplane software. Quantitative analysis of valve numbers and the shape and orientation of Prox1^{high} nuclei were done using Image J software (see details in Supplemental Experimental Procedures).

For the measurement of VE-cadherin at LEC junctions, thresholding, and quantification of the images were performed using MetaMorph Imaging software (Molecular Devices). An inclusive threshold was applied to the VE-cadherin channel in the entire tile scan image such that minimum intensity threshold values do not include background signal. Quantification of

VE-cadherin intensity for each junction area was performed from three independent experiments (in total 116 junctions for control and 134 for Celsr1-positive junctions were analyzed). PECAM-1 staining was used as reference of overlapping membrane contacts.

Serial Section Light Microscopy

The intestines of E17.5 *Prox1-CreER^{T2};R26-mTmG* mice were dissected and immediately fixed in 4% PFA/2.5% glutaraldehyde in 0.1 M phosphate buffer (pH 7.4). Samples were analyzed under a fluorescence stereomicroscope (Leica MZ16F) to localize ring-shaped valves and postfixed in reduced osmium tetroxide for 1 hr, followed by 1% tannic acid in 0.05 M sodium cacodylate for 45 min. Samples were then dehydrated through a graded series of ethanol and embedded in either Araldite or Epon resin. The same processing was used for mesenteric lymphatic vessels of P6 mice. Semi-thin sections (400 nm) were cut on a UCT ultramicrotome (Leica Microsystems UK), stained with 1% toluidine blue in 1% Borax, and viewed under a III RS light microscope (Carl Zeiss UK) to locate the area of interest. For 3D reconstruction, images of serial semi-thin sections (400 nm) through the developing valve were aligned, segmented, and rendered in Amira software (Visage Imaging).

Electron Microscopy

Ultrathin sections of 70–80 nm were cut from araldite or Epon-embedded samples (prepared as described above) and poststained with lead citrate. Images were obtained with a JEOL 1010 transmission electron microscope and Bioscan CCD camera (Gatan UK), or a Tecnai G2 Spirit transmission electron microscope (FEI Company) and Orius CCD camera (Gatan UK).

Statistical Analysis

Statistical analysis was done using two-tailed unpaired Student's t test or Mann-Whitney test as indicated in the legends for Figures 3F, 4E, 4K, 6F, and 6G.

SUPPLEMENTAL INFORMATION

Supplemental Information includes Supplemental Experimental Procedures, seven figures, and four movies and can be found with this article online at http://dx.doi.org/10.1016/j.devcel.2013.05.015.

ACKNOWLEDGMENTS

We thank Jennifer Murdoch for *Crsh* embryos, Dawn Savery and Andrew Copp for *Looptail* mice, Mireille Montcouquiol for Vangl2 antibodies, Lydia Sorokin for Laminin-α5 antibodies, and Tatiana Petrova for Prox1-GST construct. We would also like to thank Martin Jones for MATLAB analysis, Sherry Xie for help with the mice and for generating the Prox1 antibody, and the animal unit staff at the London Research Institute for animal husbandry. This work was supported by Cancer Research UK (to F. Tatin, A.T., A.W., and T.M.), the EMBO Young Investigator Programme (to T.M.), grant R01-AR27883 from the National Institutes of Health (to E.F.), FRSM 3.4550.11 (ARC-10/15-026), and the Fondation Médicale Reine Elisabeth (to F. Tissir).

Received: December 14, 2012
Revised: April 23, 2013
Accepted: May 14, 2013
Published: June 20, 2013

REFERENCES

Alitalo, K. (2011). The lymphatic vasculature in disease. Nat. Med. *17*, 1371–1380.

Bastock, R., and Strutt, D. (2007). The planar polarity pathway promotes coordinated cell migration during Drosophila oogenesis. Development *134*, 3055–3064.

Bazigou, E., and Makinen, T. (2012). Flow control in our vessels: vascular valves make sure there is no way back. Cell. Mol. Life Sci. *70*, 1055–1066.

Bazigou, E., Xie, S., Chen, C., Weston, A., Miura, N., Sorokin, L., Adams, R., Muro, A.F., Sheppard, D., and Makinen, T. (2009). Integrin-alpha9 is required for fibronectin matrix assembly during lymphatic valve morphogenesis. Dev. Cell *17*, 175–186.

Bazigou, E., Lyons, O.T., Smith, A., Venn, G.E., Cope, C., Brown, N.A., and Makinen, T. (2011). Genes regulating lymphangiogenesis control venous valve formation and maintenance in mice. J. Clin. Invest. *121*, 2984–2992.

Bertet, C., Sulak, L., and Lecuit, T. (2004). Myosin-dependent junction remodelling controls planar cell intercalation and axis elongation. Nature *429*, 667–671.

Blum, Y., Belting, H.G., Ellertsdottir, E., Herwig, L., Lüders, F., and Affolter, M. (2008). Complex cell rearrangements during intersegmental vessel sprouting and vessel fusion in the zebrafish embryo. Dev. Biol. *316*, 312–322.

Bose, R., and Wrana, J.L. (2006). Regulation of Par6 by extracellular signals. Curr. Opin. Cell Biol. *18*, 206–212.

Carreira-Barbosa, F., Kajita, M., Morel, V., Wada, H., Okamoto, H., Martinez Arias, A., Fujita, Y., Wilson, S.W., and Tada, M. (2009). Flamingo regulates epiboly and convergence/extension movements through cell cohesive and signalling functions during zebrafish gastrulation. Development *136*, 383–392.

Chen, P.L., and Clandinin, T.R. (2008). The cadherin Flamingo mediates level-dependent interactions that guide photoreceptor target choice in Drosophila. Neuron *58*, 26–33.

Ciruna, B., Jenny, A., Lee, D., Mlodzik, M., and Schier, A.F. (2006). Planar cell polarity signalling couples cell division and morphogenesis during neurulation. Nature *439*, 220–224.

Curtin, J.A., Quint, E., Tsipouri, V., Arkell, R.M., Cattanach, B., Copp, A.J., Henderson, D.J., Spurr, N., Stanier, P., Fisher, E.M., et al. (2003). Mutation of Celsr1 disrupts planar polarity of inner ear hair cells and causes severe neural tube defects in the mouse. Curr. Biol. *13*, 1129–1133.

Dejana, E., and Giampietro, C. (2012). Vascular endothelial-cadherin and vascular stability. Curr. Opin. Hematol. *19*, 218–223.

Devenport, D., and Fuchs, E. (2008). Planar polarization in embryonic epidermis orchestrates global asymmetric morphogenesis of hair follicles. Nat. Cell Biol. *10*, 1257–1268.

Dzamba, B.J., Jakab, K.R., Marsden, M., Schwartz, M.A., and DeSimone, D.W. (2009). Cadherin adhesion, tissue tension, and noncanonical Wnt signaling regulate fibronectin matrix organization. Dev. Cell *16*, 421–432.

Ewald, A.J., Huebner, R.J., Palsdottir, H., Lee, J.K., Perez, M.J., Jorgens, D.M., Tauscher, A.N., Cheung, K.J., Werb, Z., and Auer, M. (2012). Mammary collective cell migration involves transient loss of epithelial features and individual cell migration within the epithelium. J. Cell Sci. *125*, 2638–2654.

Formstone, C.J., and Mason, I. (2005). Combinatorial activity of Flamingo proteins directs convergence and extension within the early zebrafish embryo via the planar cell polarity pathway. Dev. Biol. *282*, 320–335.

Gaengel, K., Niaudet, C., Hagikura, K., Laviña, B., Muhl, L., Hofmann, J.J., Ebarasi, L., Nyström, S., Rymo, S., Chen, L.L., et al. (2012). The sphingosine-1-phosphate receptor S1PR1 restricts sprouting angiogenesis by regulating the interplay between VE-cadherin and VEGFR2. Dev. Cell *23*, 587–599.

Gao, F.B., Kohwi, M., Brenman, J.E., Jan, L.Y., and Jan, Y.N. (2000). Control of dendritic field formation in Drosophila: the roles of flamingo and competition between homologous neurons. Neuron *28*, 91–101.

Glasco, D.M., Sittaramane, V., Bryant, W., Fritzsch, B., Sawant, A., Paudyal, A., Stewart, M., Andre, P., Cadete Vilhais-Neto, G., Yang, Y., et al. (2012). The mouse Wnt/PCP protein Vangl2 is necessary for migration of facial branchiomotor neurons, and functions independently of Dishevelled. Dev. Biol. *369*, 211–222.

Gomez, G.A., McLachlan, R.W., and Yap, A.S. (2011). Productive tension: force-sensing and homeostasis of cell-cell junctions. Trends Cell Biol. *21*, 499–505.

Goodrich, L.V., and Strutt, D. (2011). Principles of planar polarity in animal development. Development *138*, 1877–1892.

Gray, R.S., Roszko, I., and Solnica-Krezel, L. (2011). Planar cell polarity: coordinating morphogenetic cell behaviors with embryonic polarity. Dev. Cell *21*, 120–133.

Hakeda-Suzuki, S., Berger-Müller, S., Tomasi, T., Usui, T., Horiuchi, S.Y., Uemura, T., and Suzuki, T. (2011). Golden Goal collaborates with Flamingo

in conferring synaptic-layer specificity in the visual system. Nat. Neurosci. *14*, 314–323.

Halbleib, J.M., and Nelson, W.J. (2006). Cadherins in development: cell adhesion, sorting, and tissue morphogenesis. Genes Dev. *20*, 3199–3214.

Iden, S., Rehder, D., August, B., Suzuki, A., Wolburg-Buchholz, K., Wolburg, H., Ohno, S., Behrens, J., Vestweber, D., and Ebnet, K. (2006). A distinct PAR complex associates physically with VE-cadherin in vertebrate endothelial cells. EMBO Rep. *7*, 1239–1246.

Jakobsson, L., Franco, C.A., Bentley, K., Collins, R.T., Ponsioen, B., Aspalter, I.M., Rosewell, I., Busse, M., Thurston, G., Medvinsky, A., et al. (2010). Endothelial cells dynamically compete for the tip cell position during angiogenic sprouting. Nat. Cell Biol. *12*, 943–953.

Kametani, Y., and Takeichi, M. (2007). Basal-to-apical cadherin flow at cell junctions. Nat. Cell Biol. *9*, 92–98.

Kibar, Z., Vogan, K.J., Groulx, N., Justice, M.J., Underhill, D.A., and Gros, P. (2001). Ltap, a mammalian homolog of Drosophila Strabismus/Van Gogh, is altered in the mouse neural tube mutant Loop-tail. Nat. Genet. *28*, 251–255.

Lee, R.C., Clandinin, T.R., Lee, C.H., Chen, P.L., Meinertzhagen, I.A., and Zipursky, S.L. (2003). The protocadherin Flamingo is required for axon target selection in the Drosophila visual system. Nat. Neurosci. *6*, 557–563.

Matsubara, D., Horiuchi, S.Y., Shimono, K., Usui, T., and Uemura, T. (2011). The seven-pass transmembrane cadherin Flamingo controls dendritic self-avoidance via its binding to a LIM domain protein, Espinas, in Drosophila sensory neurons. Genes Dev. *25*, 1982–1996.

Montcouquiol, M., Rachel, R.A., Lanford, P.J., Copeland, N.G., Jenkins, N.A., and Kelley, M.W. (2003). Identification of Vangl2 and Scrb1 as planar polarity genes in mammals. Nature *423*, 173–177.

Muzumdar, M.D., Tasic, B., Miyamichi, K., Li, L., and Luo, L. (2007). A global double-fluorescent Cre reporter mouse. Genesis *45*, 593–605.

Nambiar, R.M., Ignatius, M.S., and Henion, P.D. (2007). Zebrafish colgate/hdac1 functions in the non-canonical Wnt pathway during axial extension and in Wnt-independent branchiomotor neuron migration. Mech. Dev. *124*, 682–698.

Nishimura, T., Honda, H., and Takeichi, M. (2012). Planar cell polarity links axes of spatial dynamics in neural-tube closure. Cell *149*, 1084–1097.

Norrmén, C., Ivanov, K.I., Cheng, J., Zangger, N., Delorenzi, M., Jaquet, M., Miura, N., Puolakkainen, P., Horsley, V., Hu, J., et al. (2009). FOXC2 controls formation and maturation of lymphatic collecting vessels through cooperation with NFATc1. J. Cell Biol. *185*, 439–457.

Petrova, T.V., Mäkinen, T., Mäkelä, T.P., Saarela, J., Virtanen, I., Ferrell, R.E., Finegold, D.N., Kerjaschki, D., Ylä-Herttuala, S., and Alitalo, K. (2002). Lymphatic endothelial reprogramming of vascular endothelial cells by the Prox-1 homeobox transcription factor. EMBO J. *21*, 4593–4599.

Qu, Y., Glasco, D.M., Zhou, L., Sawant, A., Ravni, A., Fritzsch, B., Damrau, C., Murdoch, J.N., Evans, S., Pfaff, S.L., et al. (2010). Atypical cadherins Celsr1-3 differentially regulate migration of facial branchiomotor neurons in mice. J. Neurosci. *30*, 9392–9401.

Sabine, A., Agalarov, Y., Maby-El Hajjami, H., Jaquet, M., Hägerling, R., Pollmann, C., Bebber, D., Pfenniger, A., Miura, N., Dormond, O., et al. (2012). Mechanotransduction, PROX1, and FOXC2 cooperate to control connexin37 and calcineurin during lymphatic-valve formation. Dev. Cell *22*, 430–445.

Seifert, J.R., and Mlodzik, M. (2007). Frizzled/PCP signalling: a conserved mechanism regulating cell polarity and directed motility. Nat. Rev. Genet. *8*, 126–138.

Shafer, B., Onishi, K., Lo, C., Colakoglu, G., and Zou, Y. (2011). Vangl2 promotes Wnt/planar cell polarity-like signaling by antagonizing Dvl1-mediated feedback inhibition in growth cone guidance. Dev. Cell *20*, 177–191.

Sittaramane, V., Sawant, A., Wolman, M.A., Maves, L., Halloran, M.C., and Chandrasekhar, A. (2009). The cell adhesion molecule Tag1, transmembrane protein Stbm/Vangl2, and Lamininalpha1 exhibit genetic interactions during migration of facial branchiomotor neurons in zebrafish. Dev. Biol. *325*, 363–373.

Strutt, D.I. (2001). Asymmetric localization of frizzled and the establishment of cell polarity in the Drosophila wing. Mol. Cell *7*, 367–375.

Strutt, H., Warrington, S.J., and Strutt, D. (2011). Dynamics of core planar polarity protein turnover and stable assembly into discrete membrane subdomains. Dev. Cell *20*, 511–525.

Tada, M., and Smith, J.C. (2000). Xwnt11 is a target of Xenopus Brachyury: regulation of gastrulation movements via Dishevelled, but not through the canonical Wnt pathway. Development *127*, 2227–2238.

Tissir, F., Bar, I., Jossin, Y., De Backer, O., and Goffinet, A.M. (2005). Protocadherin Celsr3 is crucial in axonal tract development. Nat. Neurosci. *8*, 451–457.

Usui, T., Shima, Y., Shimada, Y., Hirano, S., Burgess, R.W., Schwarz, T.L., Takeichi, M., and Uemura, T. (1999). Flamingo, a seven-pass transmembrane cadherin, regulates planar cell polarity under the control of Frizzled. Cell *98*, 585–595.

Wada, H., Tanaka, H., Nakayama, S., Iwasaki, M., and Okamoto, H. (2006). Frizzled3a and Celsr2 function in the neuroepithelium to regulate migration of facial motor neurons in the developing zebrafish hindbrain. Development *133*, 4749–4759.

Wallingford, J.B., Rowning, B.A., Vogeli, K.M., Rothbächer, U., Fraser, S.E., and Harland, R.M. (2000). Dishevelled controls cell polarity during Xenopus gastrulation. Nature *405*, 81–85.

Zhou, L., Bar, I., Achouri, Y., Campbell, K., De Backer, O., Hebert, J.M., Jones, K., Kessaris, N., de Rouvroit, C.L., O'Leary, D., et al. (2008). Early forebrain wiring: genetic dissection using conditional Celsr3 mutant mice. Science *320*, 946–949.